

Pulsed-incoherent-light-injected Fabry-Perot laser diode for WDM passive optical networks

Hoon Kim

Dept. of Electrical & Computer Engineering, National University of Singapore, 4 Engineering Drive 3, Singapore 117576, hoonkim@ieee.org

Abstract: We propose and demonstrate a pulsed-incoherent-light-injected Fabry-Perot laser diode (FP-LD) which generates incoherent return-to-zero (RZ) signals for wavelength-division-multiplexing passive optical networks. For the generation of the RZ signals, we first convert the continuous-wave (CW) amplified spontaneous emission (ASE) into an ASE pulse train with a pulse carver, spectrum-slice it into multiple channels with a waveguide grating router, and then inject them into FP-LDs for data modulation. Thanks to a wide slicing bandwidth of the injected incoherent light, the spectral linewidth of the generated RZ signals is determined by the slicing bandwidth, without being affected by the use of the RZ format. Thus, compared to incoherent non-return-to-zero (NRZ) signals generated with CW-ASE-injected FP-LDs, the RZ signals have a similar spectral linewidth but a wide timing margin between adjacent bits. Thus, the proposed transmitter can offer better dispersion tolerance than the NRZ signals. For example, our experimental demonstration performed at 1.25 Gb/s shows ~50% higher dispersion tolerance than the NRZ signals generated with CW ASE-injected FP-LDs. Despite the large slicing bandwidth of 0.67 nm for the injected ASE, we were able to transmit 1.25-Gb/s signals over 45-km standard single-mode fiber without dispersion compensation. The receiver sensitivity is also improved by 1.5 dB by using the RZ format.

©2010 Optical Society of America

OCIS codes: (060.0060) Fiber optics and optical communications; (060.2330) Fiber optics communications

References and links

1. H. D. Kim, S.-G. Kang, and C.-H. Lee, "A low-cost WDM source with an ASE injected Fabry-Perot semiconductor laser," *IEEE Photon. Technol. Lett.* **12**(8), 1067–1069 (2000).
2. D. J. Shin, D. K. Jung, H. S. Shin, J. W. Kwon, S. Hwang, Y. Oh, and C. Shim, "Hybrid WDM/TDM-PON with wavelength-selection-free transmitters," *J. Lightwave Technol.* **23**(1), 187–195 (2005).
3. K.-Y. Park, S.-G. Mun, K.-M. Choi, and C.-H. Lee, "A theoretical model of a wavelength-locked Fabry-Perot laser diode to the externally injected narrow-band ASE," *IEEE Photon. Technol. Lett.* **17**(9), 1797–1799 (2005).
4. D. J. Shin, Y. C. Keh, J. W. Kwon, E. H. Lee, J. K. Lee, and M. K. Park, "J. W. Park, Y. K. Oh, S. W. Kim, I. K. Yun, H. C. Shin, D. Heo, J. S. Lee, H. S. Shin, H. S. Kim, S. B. Park, D. K. Jung, S. Hwang, Y. J. Oh, D. H. Jang, and C. S. Shim, "Low-cost WDM-PON with colorless bidirectional transceivers," *J. Lightwave Technol.* **24**(1), 158–165 (2006).
5. S.-M. Lee, S.-G. Mun, M.-H. Kim, and C.-H. Lee, "Demonstration of a long-reach DWDM-PON for consolidation of metro and access networks," *J. Lightwave Technol.* **25**(1), 271–276 (2007).
6. S.-G. Mun, J.-H. Moon, H.-K. Lee, J.-Y. Kim, and C.-H. Lee, "A WDM-PON with a 40 Gb/s (32 x 1.25 Gb/s) capacity based on wavelength-locked Fabry-Perot laser diodes," *Opt. Express* **16**(15), 11361–11368 (2008).
7. C. H. Kim, K. Lee, and S. B. Lee, "Effects of in-band crosstalk in wavelength-locked Fabry-Perot laser diode-based WDM PONs," *IEEE Photon. Technol. Lett.* **21**(9), 596–598 (2009).
8. Y. S. Jang, C.-H. Lee, and Y. Chung, "Effects of crosstalk in WDM systems using spectrum-sliced light source," *IEEE Photon. Technol. Lett.* **11**(6), 715–717 (1999).
9. H. Kim, H. C. Ji, and C. H. Kim, "Effects of intraband crosstalk on incoherent light using SOA-based noise suppression technique," *IEEE Photon. Technol. Lett.* **18**(14), 1542–1544 (2006).
10. F. Forghieri, P. Prucnal, R. Tkach, and A. Chraplyvy, "RZ versus NRZ in nonlinear WDM systems," *IEEE Photon. Technol. Lett.* **9**(7), 1035–1037 (1997).
11. F. Heismann, "Origin of clock-frequency components in NRZ-formatted optical signals," *IEEE Photon. Technol. Lett.* **15**(7), 912–914 (2003).

12. L. Hou, H. Zhu, F. Zhou, L. Wang, J. Bian, and W. Wang, "Monolithically integrated semiconductor optical amplifier and electroabsorption modulator with dual-waveguide spot-size converter input and output," *Semicond. Sci. Technol.* **20**(9), 912–916 (2005).
13. N. M. Froberg, G. Raybon, U. Koren, B. I. Miller, M. G. Young, M. Chien, G. T. Harvey, A. Gnauck, and A. M. Johnson, "Generation of 12.5 Gbit/s soliton data stream with an integrated laser-modulator transmitter," *Electron. Lett.* **30**(22), 1880–1881 (1994).
14. D. J. Shin, D. K. Jung, J. K. Lee, J. H. Lee, Y. H. Choi, Y. C. Band, H. S. Shin, J. Lee, S. T. Hwang, and Y. J. Oh, "155 Mbit/s transmission using ASE-injected Fabry-Perot laser diode in WDM-PON over 70°C temperature range," *Electron. Lett.* **39**(18), 1331–1332 (2003).
15. M. J. Munroe, J. Cooper, and M. G. Raymer, "Spectral broadening of stochastic light intensity-smoothed by a saturated semiconductor optical amplifier," *IEEE J. Quantum Electron.* **34**(3), 548–551 (1998).
16. A. D. McCoy, P. Horak, B. C. Thomsen, M. Ibsen, and D. J. Richardson, "Noise suppression of incoherent light using a gain-saturated SOA: implications for spectrum-sliced WDM systems," *J. Lightwave Technol.* **23**(8), 2399–2409 (2005).
17. H. Kim, S. Kim, S. Hwang, and Y. Oh, "Impact of dispersion, PMD, and PDL on the performance of spectrum-sliced incoherent light sources using gain-saturated semiconductor optical amplifiers," *J. Lightwave Technol.* **24**(2), 775–785 (2006).

1. Introduction

Incoherent-light-injected Fabry-Perot laser diodes (FP-LDs) have attracted lots of attention as cost-effective optical sources for wavelength-division-multiplexing (WDM) passive optical networks (PONs) [1]-[7]. This is because not only are FP-LDs semiconductor devices with simple structure and high yield, but also their operating wavelength is determined by the wavelength of the injected light. Thus, the compact and low-cost light sources allow all optical transmitters to be used interchangeably for any WDM channels, enabling colorless operation in the network. Moreover, the incoherent nature of the output light greatly enhances the robustness against in-band optical crosstalk possibly caused by optical reflection and Rayleigh backscattering [7]-[9]. This merit is especially beneficial when they are used for single-fiber-based long-reach PON systems. However, major drawbacks of incoherent-light-injected FP-LDs are high susceptibility to fiber dispersion and poor receiver sensitivity. These should be attributed to wide spectral linewidth of the output light and large excess intensity noise (EIN) of the injected incoherent light, respectively.

In this paper, we propose and demonstrate a pulsed-incoherent-light injection scheme to improve the dispersion tolerance of incoherent-light-injected FP-LDs. By injecting a pulse train of incoherent light into an FP-LD driven by electrical non-return-to-zero (NRZ) signals, we generate return-to-zero (RZ) signals at the output of the FP-LD. It is well-known that for coherent light the RZ format is less tolerant to fiber dispersion than the NRZ format [9]. This is simply because the RZ format has wider spectral linewidth than the NRZ. For spectrum-sliced incoherent light, on the other hand, the spectral linewidth is determined by the slicing bandwidth rather than which modulation format is used. Thus, the RZ format, which offers a large timing margin between adjacent bits, can be more tolerant to dispersion-induced pulse broadening than the NRZ format for incoherent light. The use of RZ format also improves the receiver sensitivity by 2 dB for PIN detector [10]. Another advantage of the RZ format over the NRZ is easy clock recovery. Unlike NRZ signals [11], RZ signals have a strong clock tone in their electrical spectrum and it facilitates the clock recovery. We show through our experimental demonstration performed at 1.25 Gb/s that the proposed RZ transmitter has ~50% higher dispersion tolerance than the NRZ counterpart without changing the spectral properties of incoherent-light-injected FP-LDs. The improvement in receiver sensitivity is measured to be 1.5 dB.

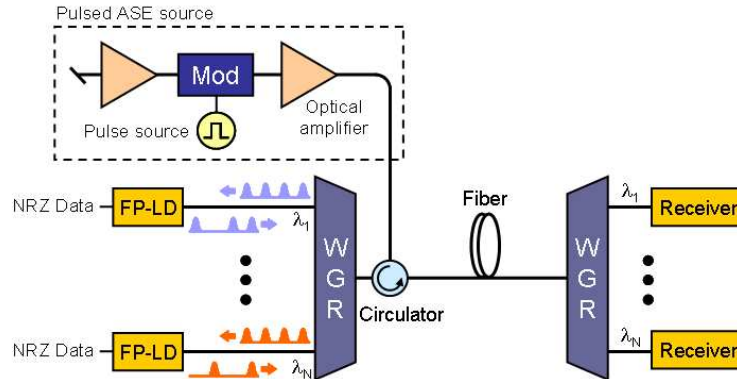


Fig. 1. Pulsed-incoherent-light-injected FP-LDs for WDM-PON systems.

2. Pulsed-incoherent-light-injected FP-LDs

Figure 1 shows a schematic diagram of the proposed scheme. The pulsed amplified spontaneous emission (ASE) source is composed of an ASE source and a pulse carver. The ASE source can be Erbium-doped fiber amplifiers (EDFAs) and/or semiconductor optical amplifiers (SOAs) with no input signals [4]. If the semiconductor-based optical amplifiers are used, an electro-absorption modulator (EAM) is preferable to a Mach-Zehnder modulator as a pulse carver for monolithic integration with the amplifiers [12]. The pulse carver is driven with a clock signal. The generated ASE pulse train is fed to a circulator followed by a waveguide grating router (WGR) for spectrum slicing. The spectrum-sliced incoherent pulse trains are then injected into FP-LDs for data modulation. Since the injected light is a pulse train, the FP-LD output becomes RZ signals. It is worth noting that the FP-LDs are driven with NRZ data and thus the proposed scheme does not require high modulation-bandwidth FP-LDs for RZ modulation. One easy way of generating optical RZ signals is to generate electrical RZ signals using an electrical NRZ-to-RZ converter and then apply them to an optical source [13]. In this case, however, the modulation bandwidth of the optical source should be large enough to accommodate the wide electrical spectrum of the RZ signals. Not only is it challenging to increase the modulation bandwidth of FP-LDs but it also increases the cost of the LDs and their driving circuitry. Therefore, the proposed scheme would be suitable for cost-effective RZ generation with low-bandwidth FP-LDs. The additional cost incurred by the pulse carver is shared with multiple users (i.e. N users in Fig. 1), and thus the increased cost per customer becomes insignificant as the number of users increases.

3. Experiment and results

Figure 2 shows the experimental setup. The pulsed ASE was generated with a two-stage EDFA with an EAM as an inter-stage element for pulse carving. The EAM was driven by a 1.25-GHz rectangular wave and generated a 50% duty-ratio pulse with an extinction ratio of 10 dB. The pulsed ASE was sent to an optical filter (BPF1) for spectral slicing. Figure 2(a) shows the optical spectrum of the spectrum-sliced ASE measured with an optical spectrum analyzer (resolution = 0.02 nm). The 3-dB and 10-dB bandwidths of the filter were 0.67 and 0.78 nm, respectively. The duty ratio and extinction ratio of the pulse remained unchanged after the slicing. Figure 2(b) shows the eye diagram of the injected ASE measured at the port 2 of the circulator. Due to high EIN of the incoherent light, we averaged 1024 waveforms for display. The sliced ASE was then injected to an FP-LD via a circulator. The transistor outlook (TO)-packaged and uncooled FP-LD has a mode spacing of 0.55 nm and the threshold current of 14.5 mA. To facilitate the ASE injection, the front-facet reflectivity is reduced to 1% with anti-reflection coating [2].

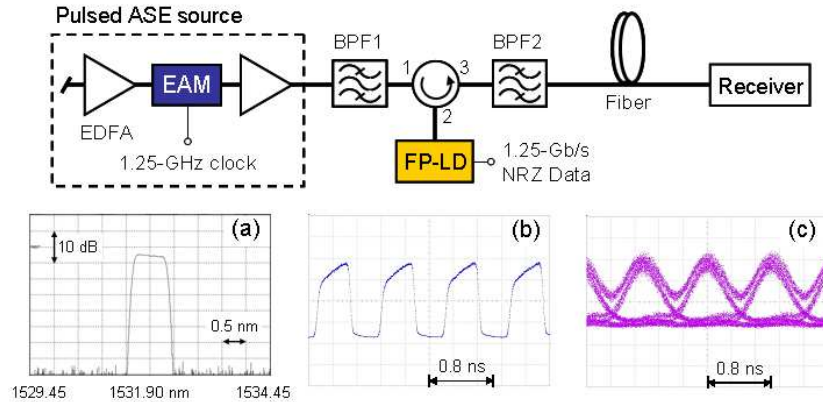


Fig. 2. Experimental setup. BPF: band-pass filter, EAM: electro-absorption modulator, EDFA: Erbium-doped fiber amplifier. (a) The optical spectrum of the spectrum-sliced ASE measured at the port 1 of the circulator. (b) The eye diagram of the pulsed ASE measured at the port 2 of the circulator. Due to excess intensity noise of the incoherent light, we averaged 1024 waveforms for display. (c) The eye diagram of the RZ signals measured at the receiver.

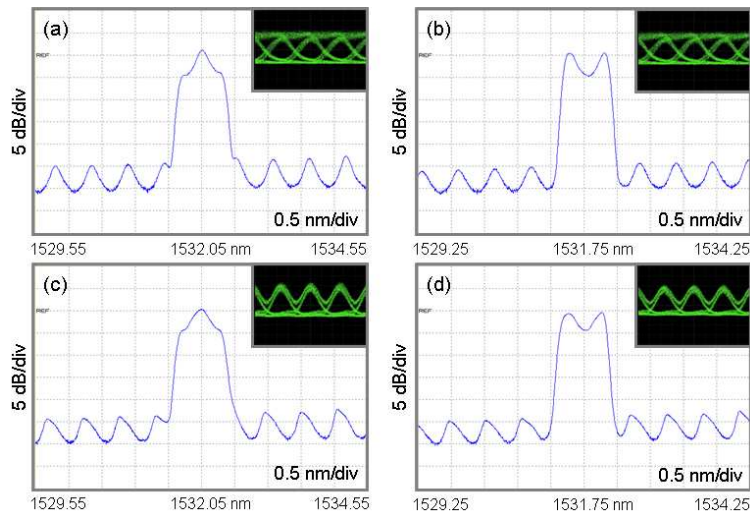


Fig. 3. Optical spectra of the FP-LD output when (a) CW ASE is injected at the peak of an FP-LD mode (A-shaped), (b) CW ASE is injected between FP-LD modes (M-shaped), (c) pulsed ASE is injected at the peak of an FP-LD mode (A-shaped), and (d) pulsed ASE is injected between FP-LD modes (M-shaped). The average optical power of the injected ASE was -13 dBm. The insets show the eye diagrams.

The FP-LD was modulated with 1.25-Gb/s NRZ signals with a pseudo-random bit sequence length of $2^{31}-1$. The bias current was set to be 18.5 mA. Before the FP-LD output was launched to standard single-mode fiber (SSMF) for transmission, the generated signals passed through another optical filter (BPF2) with a 3-dB bandwidth of 1.5 nm. This is to reject small side-modes of the FP-LD spreading over 30 nm. After transmission, the signals were detected with a PIN receiver (bandwidth = 938 MHz). Figure 2(c) shows the eye diagram of the 1.25-Gb/s RZ signals measured at the receiver. In the setup, it should be noted that we utilized two band-pass filters, one for spectrum slicing (BPF1) and the other for side-mode rejection (BPF2). This was because BPF1 was not reciprocal, but in real systems the two filters can be replaced with a single filter (e.g., WGR in Fig. 1) located at the port 2 of the circulator. Nonetheless, we believe our apparatus is sufficient to demonstrate the principle of our proposed scheme.

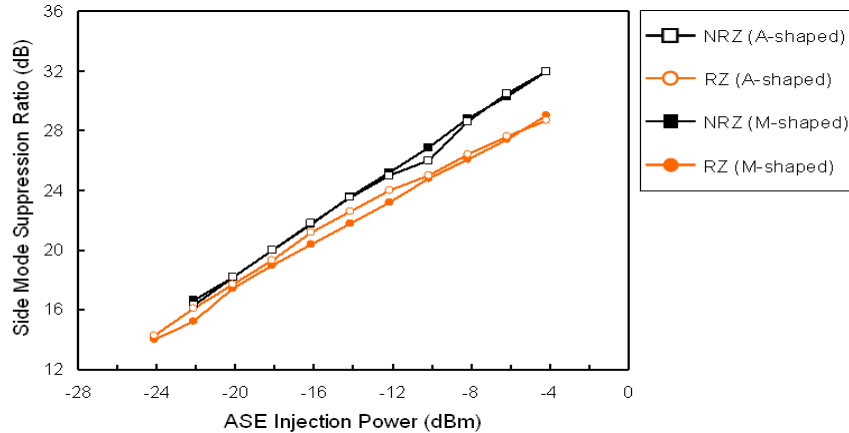


Fig. 4. Measured SMSR versus average power of the injected ASE.

Figure 3 shows the measured optical spectra of the FP-LD output when the pulsed ASE is injected and the RZ signals are generated. Also plotted in Fig. 3 for comparison are the optical spectra of continuous-wave (CW) ASE-injected FP-LD for NRZ signals. Since we choose the bandwidth of BPF1 wide enough to cover two FP-LD modes for colorless operation even with uncooled FP-LDs [14], we have two distinct output spectra, depending upon whether the ASE is injected at a peak or a valley of the FP-LD modes. When the ASE is injected at the peak of one of FP-LD modes, we have A-shaped spectra [e.g., Fig. 3(a) and (c)] whereas we have M-shaped ones [e.g., Fig. 3(b) and (d)] if the ASE is injected between the modes. The insets of Fig. 3 show the optical eye diagrams measured at the output of BPF2.

We first measured the side-mode suppression ratio (SMSR) versus the average optical power of the injected ASE. As we increase the injection power in the measurement, the peak or valley of the FP-LD modes shifts to the longer wavelength. Thus, we adjusted the injection wavelength either to the peak or valley of the modes and tried to achieve as symmetrical spectrum as possible, as shown in Fig. 3. The measured results of Fig. 4 show that the SMSR increases with the ASE injection power [1] and is unaffected by the shape of the output spectra both for the NRZ and RZ signals. However, the slope of the curves for the RZ signals is slightly gentle, compared to the one for the NRZ signals. Thus, when the ASE injection power is high, the RZ signals exhibit slightly smaller SMSR than the NRZ signals. For example, the SMSRs are measured to be 30.4 and 27.5 dB at -4 dBm injection power for the NRZ and RZ signals, respectively. We attribute this to a slightly nonlinear relationship between the SMSR and ASE input power. The SMSR curves for the CW-ASE-injected case (i.e., open and filled square symbols in Fig. 4) are not perfectly linear and their slopes are decreased as the ASE injection power increases. Thus, a high SMSR obtained by high peak power of the pulsed ASE would not completely offset a low SMSR obtained during the off-state of the pulsed ASE, making the SMSR less than the case with CW ASE injection.

Next, we measured the spectral linewidths of the RZ signals as a function of the average power of the injected ASE and compared them with those of the NRZ signals. Figure 5(a) and (b) show the linewidths measured with the optical spectrum analyzer. For M-shaped spectra, we measured 10-dB bandwidth rather than 3-dB bandwidth because of the difficulties of defining the 3-dB bandwidth. The spectral linewidths increase with the injection ASE power. This is because the amplitude-to-phase coupling which induces spectral broadening also increases with the injection power in the gain-saturated semiconductor device [15]. The results show that the RZ signals have larger spectral linewidth than the NRZ signals.

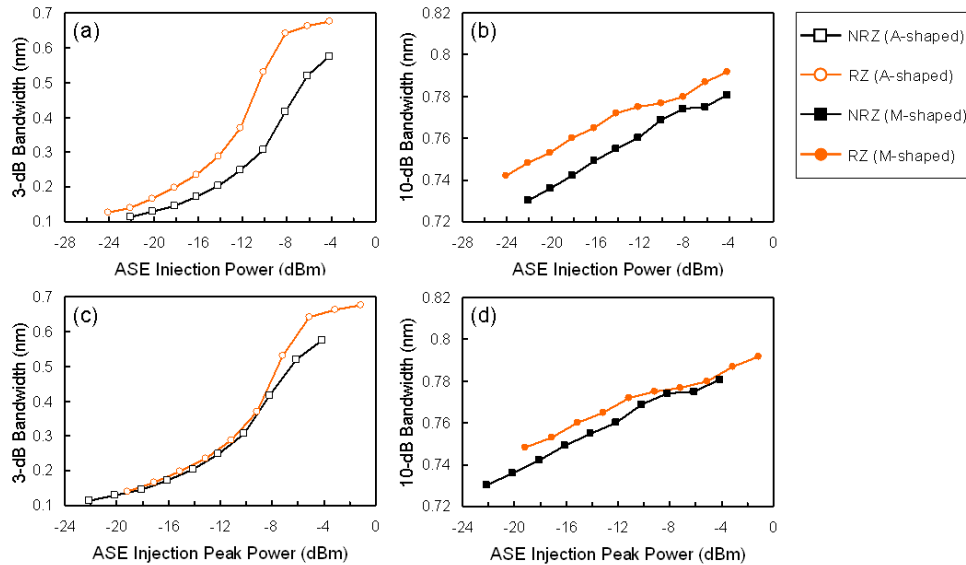


Fig. 5. Measured spectral linewidth of the FP-LD output as a function of ASE power. (a) 3-dB bandwidth of A-shaped FP-LD output, (b) 10-dB bandwidth of M-shaped FP-LD output. The same results are reproduced in (c) and (d) as a function of the peak power of the injected ASE.

To find out the reason, we reproduce the same results as a function of the *peak power* of the injected ASE in Fig. 5(c) and 5(d). Surprisingly, the two curves agree very well over most of the measured range. Thus, we can conclude that the bandwidth of ASE-injected FP-LD is mainly determined by the peak ASE power rather than the average power. It also implies that the spectral linewidth is unaffected by which modulation format is used in incoherent-light-injected FP-LDs.

Figure 6 shows the measured bit-error ratio (BER) curves for the proposed transmitter at the back-to-back transmission. For comparison, we also measured the BER curve for the NRZ signals. The average power of the injected ASE was -7 dBm. The receiver sensitivities of the RZ signals at a BER of 10^{-9} are -25.7 and -25.8 dBm for A-shaped and M-shaped signals, respectively, which are 1.3 or 1.4 dB poorer than the sensitivity measured with a directly modulated distributed-feedback laser. However, the measured receiver sensitivities of the NRZ signals are -24.5 and -24.3 dBm for A-shaped and M-shaped signals, respectively. Thus, the proposed transmitter shows ~ 1.5 dB better receiver sensitivity than the NRZ signals. Though this improvement only increases the transmission distance of power-limited systems by several kilometers, it can be used to improve the system margin and reliability.

The dispersion tolerance of the signals is measured with SSMF. Figure 7 shows the measured receiver sensitivity as a function of the transmission distance. Both for the NRZ and RZ signals, the average power of the injected ASE was -7 dBm and the output power was measured to be -3 dBm at the port 3 of the circulator. Since the FP-LD output is incoherent in nature, the chirp induced by direct modulation with FP-LD would not affect the optical properties of the signals. With the NRZ signals (i.e., open and filled square symbols in Fig. 7), we have a sensitivity penalty of ~ 4.5 dB after 30-km transmission. Obviously, this should be ascribed to inter-symbol interference (ISI) and EIN increase by dispersion [16], [17]. The electrical eye diagrams measured at the receiver in Fig. 7 show dispersion-induced pulse broadening as well as thick rails of the marks. However, when we use the RZ signals (i.e., open and filled circle symbols in Fig. 7), the similar dispersion penalty of 4.5 dB is obtained after 45-km transmission. Thus, we can achieve $\sim 50\%$ increase in dispersion-limited

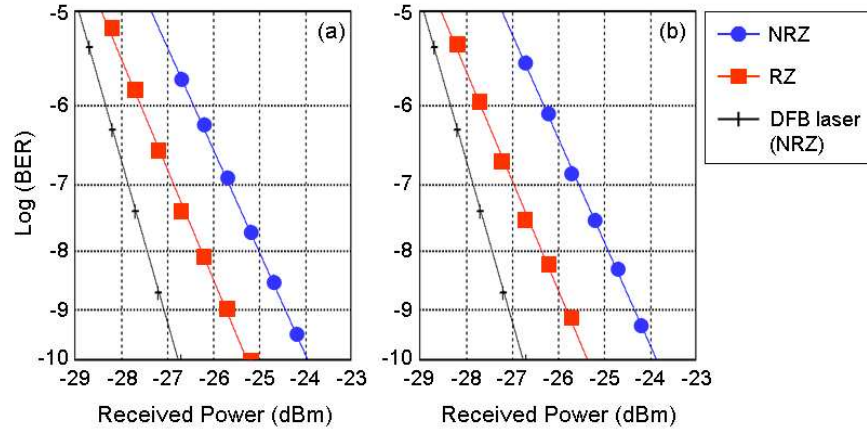


Fig. 6. Measured back-to-back receiver sensitivity for the proposed transmitter. (a) The ASE is injected at the peak of an FP-LD mode and A-shaped spectrum is generated. (b) The ASE is injected between FP-LD modes and M-shaped spectrum is generated.

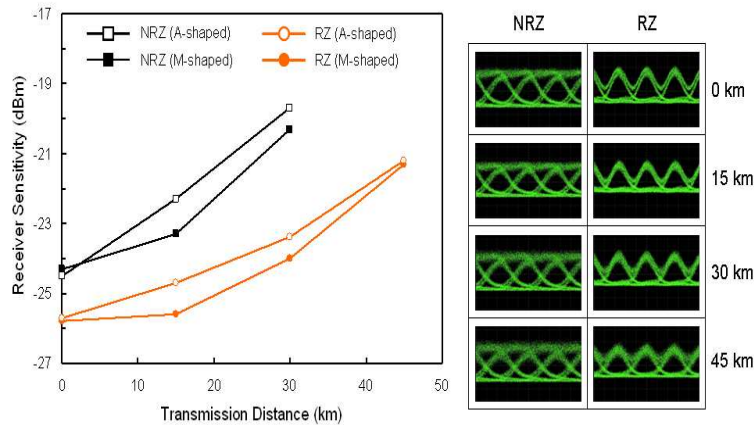


Fig. 7. Measured dispersion tolerance. The average power of the injected ASE was -7 dBm. The insets show the eye diagrams at the receivers for the M-shaped NRZ and RZ signals.

transmission distance with the RZ format. It is worth noting that this improvement is achieved with a slight increase of linewidth for the RZ signals. As shown in Fig. 5(a) and (b), the RZ signals have wider linewidth than the NRZ signals for the same average power of the injected ASE. There is no big difference between the A-shaped and M-shaped spectra in terms of dispersion tolerance. We expect the difference will be diminished if the front-facet reflectivity is further reduced at the expense of manufacturing cost.

When the proposed transmitter is used for upstream transmission, the pulsed ASE generated at the central office (CO) can suffer from fiber dispersion before it is injected into an FP-LD located at the customer's premises. In this case, we may not take advantage of using the RZ format to improve the dispersion tolerance. Large dispersion tolerance of incoherent RZ signals comes from the wide timing margin between bits since the signal occupies only a fraction of its allocated time slot. Thus, we believe that for upstream transmission low duty-ratio pulsed ASE should be launched at the CO to allow for timing margin wide enough for the RZ signals to have a roundtrip without inducing a significant ISI. The synchronization of the upstream data with pulsed ASE is also required in the proposed scheme. This can be done by first synchronizing the pulse repetition rate with the downstream data rate and then utilizing recovered the downstream clock for generating the upstream data.

4. Conclusion

We have proposed and demonstrated the pulsed-incoherent-light-injected FP-LD for WDM-PON applications. The optical transmitter generates incoherent RZ signals without increasing the spectral linewidth of the output, and thus offers higher dispersion tolerance and better receiver sensitivity than the NRZ signals generated with CW incoherent-light-injected FP-LD. Our experimental demonstration performed with 1.25-Gb/s RZ signals shows successful transmission over 45-km SSMF, which is ~50% longer than with the NRZ signals. The back-to-back receiver sensitivity is also improved by ~1.5 dB by using the RZ format. These are achieved without a significant change in side-mode suppression ratio and spectral linewidth. In WDM-PON applications, the cost of the pulsed ASE source is shared with multiple users and thus would not be significant. Therefore, we believe the proposed transmitter can be beneficial to implementing single-fiber-based long-reach WDM-PONs using incoherent light.

Acknowledgement

This work was supported by Singapore Ministry of Education Academic Research Fund Tier 1.